The Thermal Properties, Mechanical Performances and Crystallization behaviors of Poly(aryl Ether Ketone) Copolymers by the effect of Ether/Ketone Ratio

ZHIHUI HUANG[1], JIAMIAO CHEN[1], YANPING HUO[1] AND JINGWEI ZHAO[2]

[1]School of Chemical Engineering and Light Industry, Guangdong University of Technology, Guangzhou, China.

[2]Guangzhou Tinci Materials Technology Co., Ltd, Guangzhou, China.

ABSTRACT

The effect of the ether/keto ratios on the thermal properties, mechanical performances and crystallization behavior of the Poly(aryl ether ketone)s (PAEK) were investigated. A formula was proposed the estimate the melting temperatures of the PAEKs with high accuracy. Glass transition temperatures were affected by the ether/keto ratios and molecular weights, and were related with the brittle-tough transition of the PAEKs. Mechanical performances of tensile, impact, flexural and compressive strength decreased with the increase of ether/keto ratios, while elongation had a trend of increase. The non-isothermal crystallization curves exhibited well linearity when treated with Jeziorny's model, and two crystallization processes were found. The activation energies of the PAEKs were calculated to be 550~580 KJ/mol by Doyle's method. All the PAEKs exhibited spherulites and their sizes decreased with the increase of ether/keto ratios.

KEYWORDS: *Poly(aryl ether ketone), Mechanical performance, Thermal property, Crystallization behavior.*

INTRODUCTION

The poly(aryl ether ketone)s (PAEKs) are a family of thermoplastic polymers of excellent mechanical performance, chemical and thermal resistance, flame retardation, lubricating property and bio-compatibility. PAEKs can be manufactured into mechanical parts, membranes, coating and fibers through injection, 3d printing, spray coating et al.,[1-3] finding their critical applications in automobile, electronic, aerospace, energy, chemical and medical industries.[4-8] Among the PAEK family, poly(ether ether ketone) (PEEK) is the most widely

J. Polym. Mater. Vol. **38,** No. 3-4, 2021, 257-269

Correspondence author e-mail: yphuo@gdut.edu.cn
DOI : https://doi.org/10.32381/JPM.2021.38.3-4.7

available and has attracted the most research interest.

Despite PEEK has superior thermal resistance, with high melting temperature and glass transition temperature, it cannot satisfy some applications at temperature higher than 250°C (PEEK use temperature : 250°C).[9] Since the thermal resistance of PAEKs are mainly affected by the rigidity of the PAEK polymer chains, which originates from the keto bond of PAEKs, thermal resistance of PAEKs can be modified by changing the ether/keto ratios in the PAEK chains. By decreasing the ether/keto ratios, family members with higher thermal resistance like poly(ether ketone) (PEK) and poly(ether ketone ketone) (PEKK) were designed and synthesized.[10,11] The ether/keto ratios can also affect the ductility and crystallization behavior of the PAEKs, which would influence on their processability and mechanical performances. So the research of ether/keto ratios on the crystallization behavior of the PAEKs would contribute to the molecular design, manufacture and end-use of the PAEKs. Many literature on the crystallization behaviors of the PAEKs have been published, most of which focused on the crystallization behaviors of PAEK composites, substituted and cross-linked PAEKs.[12-14] However, few researches were on the intrinsic PAEKs, as well as the effect of ether/keto ratios.[15,16]

In this work, a series of PAEK copolymers with different ether/keto ratios were synthesized. The influence of ether/keto ratios on the structure, mechanical performances, thermal properties and crystallization behaviors were investigated, and efforts were made to reveal the structure-property relationship of PAEKs to help optimize their molecular design for demanding applications.

EXPERIMENTAL

Materials

4,4'-difluorobenzophenone (DFBP), hydroquinone (HQ) Diphenyl sulfone (DPS) and 4,4'-dihydroxybenzophenone (DHBP) were purchased from J&K Chemical Reagent, and all were recrystallized before use. Acetone, sodium carbonate and concentrated H_2SO_4 were purchased from Sinopharm China and used as received.

Synthesis of PAEK Copolymers

PAEKs with different ether/keto ratios were synthesized according to the polymerization recipes in Table 1. In a typical synthesis, DFBP, DHBP, HQ, Na_2CO_3 DPS were added into a flask at room temperature. The flask was then purged with nitrogen for 30 min to remove the oxygen inside. The mixture was then heated to 160°C and stirred for 1h until no more water was collected in the water separator, then it was heated to 250°C and stirred for 1h, then heated to 320°C and kept stirring. To study the kinetics of the polymerization, the reaction was terminated at a varied reaction time. Alternatively, the mixture was stirred for 6h and then poured into water immediately, and a cake with light-yellow color was collected. The cake was crashed into particles and sifted with 100 mesh sieve, followed by washing successively with three times of acetone, three times of deionized water and two times of acetone. The sample was collected and dried at 150°C in vacuum for 12h.

CHARACTERIZATION AND MEASUREMENTS

Structure and Thermal Stability

Intrinsic viscosities ([η]) of the PAEKs were determined by an Ubbelohde viscometer with a concentration of 0.5 g dL^{-1} at 25°C in concentrated sulfuric acid at 25°C. FT-IR spectra were collected on a Nicolet 6700 FT-IR spectrophotometer. Thermal degradation curves were collected on a Netzsch 209 TGA analyzer with a heating rate of 10°C min^{-1} under nitrogen atmosphere.

TABLE 1. Polymerization recipes for the PAEKs with different ether/keto ratios.

	Weight (g)				
	DFBP	DHBP	HQ	Na_2CO_3	DPS
PE_2K	43.64	0	22.02	21.41	180
$PE_{1.7}K$	43.64	7.5	18.17	21.41	180
$PE_{1.5}K$	43.64	14.35	14.64	21.41	180
$PE_{1.1}K$	43.64	35.13	3.96	21.41	180
PEK	43.64	42.84	0	21.41	180

Differential Scanning Calorimetry (DSC)

The onset temperature of the glass transition was recorded as T_g, and the peak temperature of the endothermic peak was recorded as T_m, which were detected on a DSC of TA Instrument DSC 25. For T_g and T_m, the samples were heated at 10°C/min until totally melt, kept for 5 min, then cooled to 50°C at 100°C/min, finally heated to 200°C.

For non-isothermal crystallization, the samples were heated to the temperature 20°C above T_m at 50°C/min, kept for 5min, then cooled to 200°C at cooling rates of 5, 10 and 20°C/min, respectively.

Mechanical Performances

Specimens for the mechanical performances were manufactured on an injection machine of SZS-20 (Wuhan Ruiming Instrument). Tensile, flexural and compressive tests were performed on the universal material experiment machine (CMT 4000, Shenzhen Sansi Instrument) according to the standard test methods of ISO 527, ISO 178 and ISO 604, respectively. Impact tests were performed on the impact tester (KBC 1251, Shenzhen Sansi Instrument) according to the standard test method of ISO 179.

Polarized Optical Microscopy (POM)

POM tests were performed on the PL-80 POM (Shanghai Optical Instrument) equipped with a thermal platform. The samples were molten with the thermal platform and then cooled to crystallization temperature, keeping for 60 min to complete the crystallization.

RESULTS AND DISCUSSION

Structural Validation and Polymerization Kinetics

Kinetics of the polymerization is shown in Fig. 1. It can be seen that at the polymerization time of less than 4h, [η]s of the obtained PAEKs increase rapidly as the polymerization time increasing. At the polymerization time more than 4h, their [η]s change little even if increasing polymerization time, indicating that optimum polymerization time for the synthesis of PAEKs is 6h. Meanwhile, for the same polymerization time of 6h, [η] of the PEK , $PE_{1.5}K$ and PE_2K are 1.48, 1.65 and 1.85, respectively. This can be attributed to the influence of ether and keto bonds on the solubility of PAEKs. The solubility parameters of aromatic polymers are influenced mainly by the F_{di} (molar attraction constant correlated with dispersion forces) of the aromatic repeat units and E_{hi} (cohesive energy correlated with hydrogen bonding) of the linking bonds.[17] For the PAEKs, they share the same F_{di} of 1270 $(MJ\ m^3)^{1/2}\ mol^{-1}$, while the E_{hi} ether bond and keto bond are 3000 and 2000 $J\ mol^{-1}$, thus PAEK with high ether/keto ratio would be easier to be dissolved than that of PAEK with low ether/keto ratio. Since the polymerization mechanism of PAEKs are step polymerization,

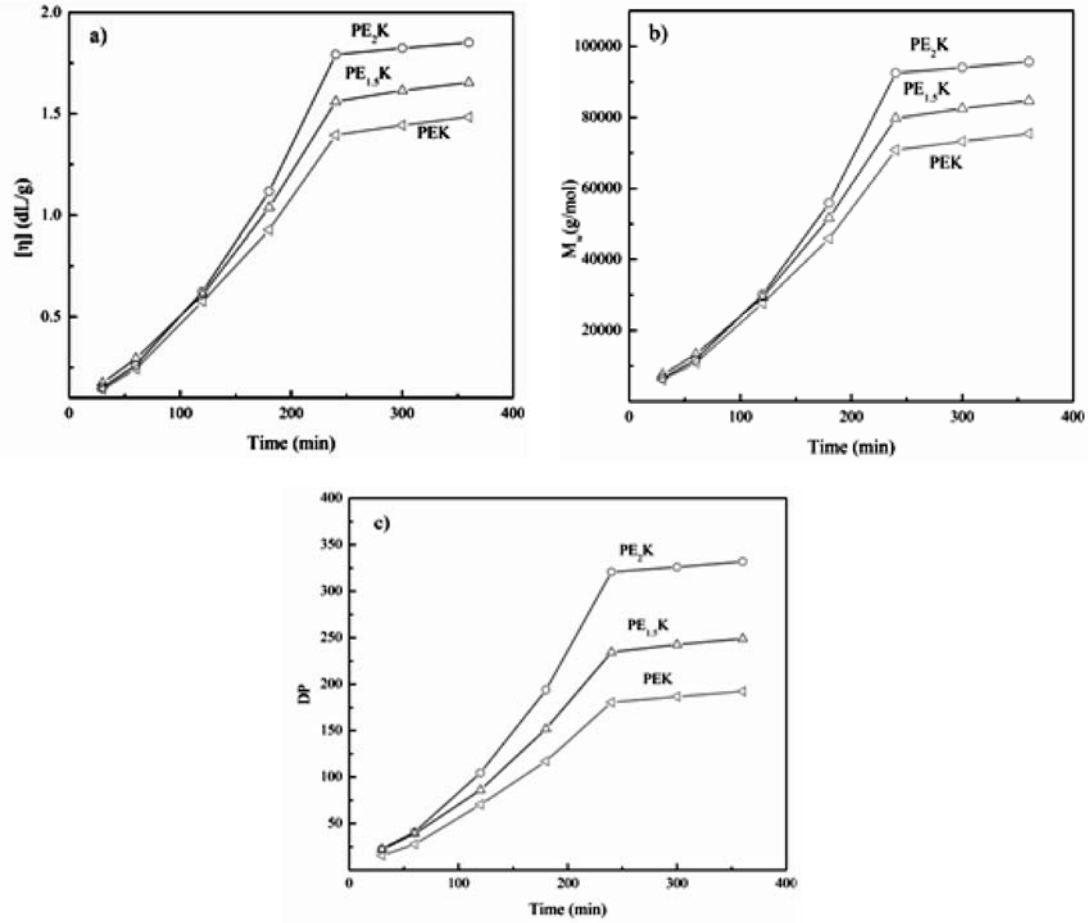

Figure 1. Kinetic of the polymerizations of at 320°C.

the reaction between the -F and -ONa group generates the chain growth of PAEKs, and for PE_2K, the higher solubility makes the -F and -ONa group on PE_2K chain easier to collide and react each other than that of $PE_{1.5}K$ and PEK, leading to a higher molecular weight.

For further investigation, molecular weights and degree of the polymerization (DP) of the PAEKs were calculated from the Mark-Houwink formula[18]:

$$[\eta]=KM^{\alpha}, \quad (1)$$

in which K is a constant, α is the expansion factor. The relationship between the polymerization time, molecular weight and DP is shown in Fig. 1b and Fig. 1c. It can be seen for all the polymerization, oligomers with DP about 20 were formed at the polymerization time of 30 min, and at the polymerization time of 6h, DPs of PE_2K, $PE_{1.5}K$ and PEK were 330, 250 and 190, respectively, indicating great

influence of ether/keto ratios.

The structures of PAEKs were confirmed by FT-IR spectra shown in Fig. 2. The peaks at 1653, 1010, 1496 and 1310 cm^{-1} were assigned to the stretching mode of C=O, in-plane bending mode of aromatic ether, in-plane vibration modes of R-O-R benzene ring and R-CO-R benzene ring, which confirmed the ether or keto connected phenyl ring structure of the polymers. Additionally, the absorption at 845 cm^{-1} was attributed to the para-substituted phenyl ring, which further confirmed the structures of PAEKs.[19]

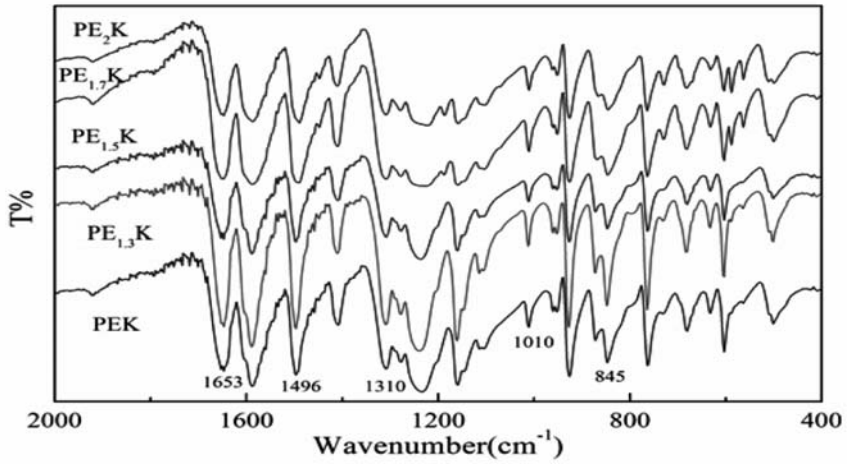

Figure 2. FT-IR spectra of the PAEKs with different ether/keto ratios synthesized at the polymerization time of 6h at 320°C

Mechanical Performances

Mechanical performances of the PAEKs obtained after 6h of polymerization are shown

TABLE 2. Mechanical performances of the PAEKs with different ether/keto ratios synthesized at the polymerization time of 6h at 320°C.

		PE_2K	$PE_{1.7}K$	$PE_{1.5}K$	$PE_{1.3}K$	$PE_{1.1}K$	PEK
[η] (dL/g)		1.85	1.72	1.65	1.60	1.45	1.48
Tensile	Strength (MPa)	95±1.5	97±2.0	100±2.5	102±2.1	105±2.5	105±2.2
	Modulus (GPa)	3.9	4.1	4.2	4.2	4.3	4.3
Flexural	Strength (MPa)	145±3.5	152±2.7	157±3.7	160±3.2	162±2.9	162±2.2
	Modulus (GPa)	3.8	4.0	4.2	4.3	4.4	4.4
Impact	Notched (KJ/m^2)	9±1.2	9±1.5	10±1.4	11±1.4	12±1.5	12±1.5
	Unnotched (KJ/m^2)	not break	not break	not break	not break	not break	not break
Compressive strength (MPa)		118±3.3	120±2.4	124±3.5	125±2.2	128±1.7	127±3.7

in Table 2. It can be seen all the PAEKs exhibit outstanding performances in tensile, flexural, impact and compressive properties. Moreover, with the decrease of ether/keto ratio, the strength and modulus increase slightly, indicating that a lower ether/keto ratio in the PAEK would make it more difficult to generate deformation. Strain-stress curves of the PAEKs are shown in Fig. 3, elongation at break increase significantly with the increase of ether/keto ratio, which can be attributed to the decrease of rigid keto bond in the PAEKs.

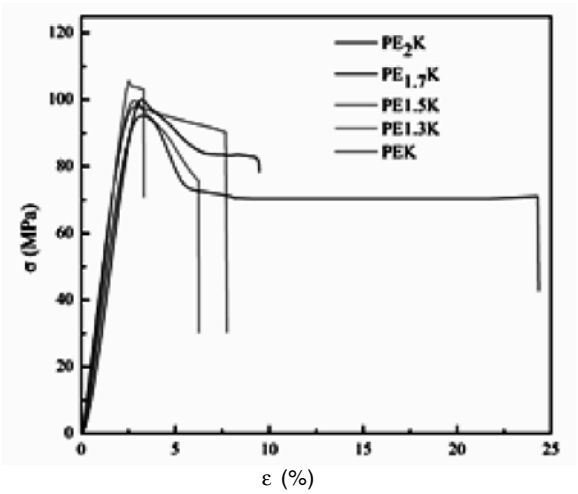

Figure 3. Strain-stress curves of the PAEKs with different ether/keto ratios synthesized at the polymerization of 6h at 320°C.

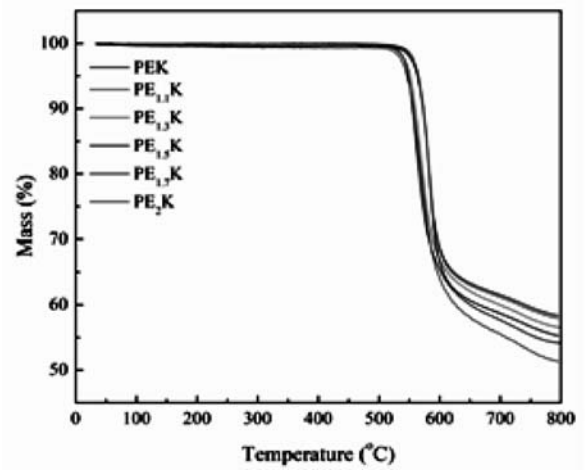

Figure 4. TG curves of the PAEKs with different ether/keto ratios synthesized at the polymerization time of 6h at 320°C.

Thermal Properties

Thermal stability of the PAEKs is shown in Fig. 4, their pyrolysis temperatures at 5% weight loss ($T_{5\%}$) and pyrolysis temperatures at maximum pyrolysis rate (T_{max}) are summarized in Table 3. All the PAEKs show excellent thermal stability, with $T_{5\%}$ higher than 500°C and T_{max} higher than 550°C. Additionally, $T_{5\%}$ of the PAEKs decrease slightly with the increase of ether/keto ratios, indicating that the scission rate of ether group above 500°C is higher than that of keto group.[20]

Melting curves of the PAEKs are shown in Fig. 5a, the melting temperature (T_m), and heat of fusion (ΔH_m) are summarized in Table 3. Both T_ms and ΔH_ms of the PAEKs decrease with the increase of ether/keto ratios, which is attributed to the rigidity of keto bonds. Meanwhile, molecular weights of the PAEKs had little effect on the T_ms. By fitting the T_ms with ether/keto

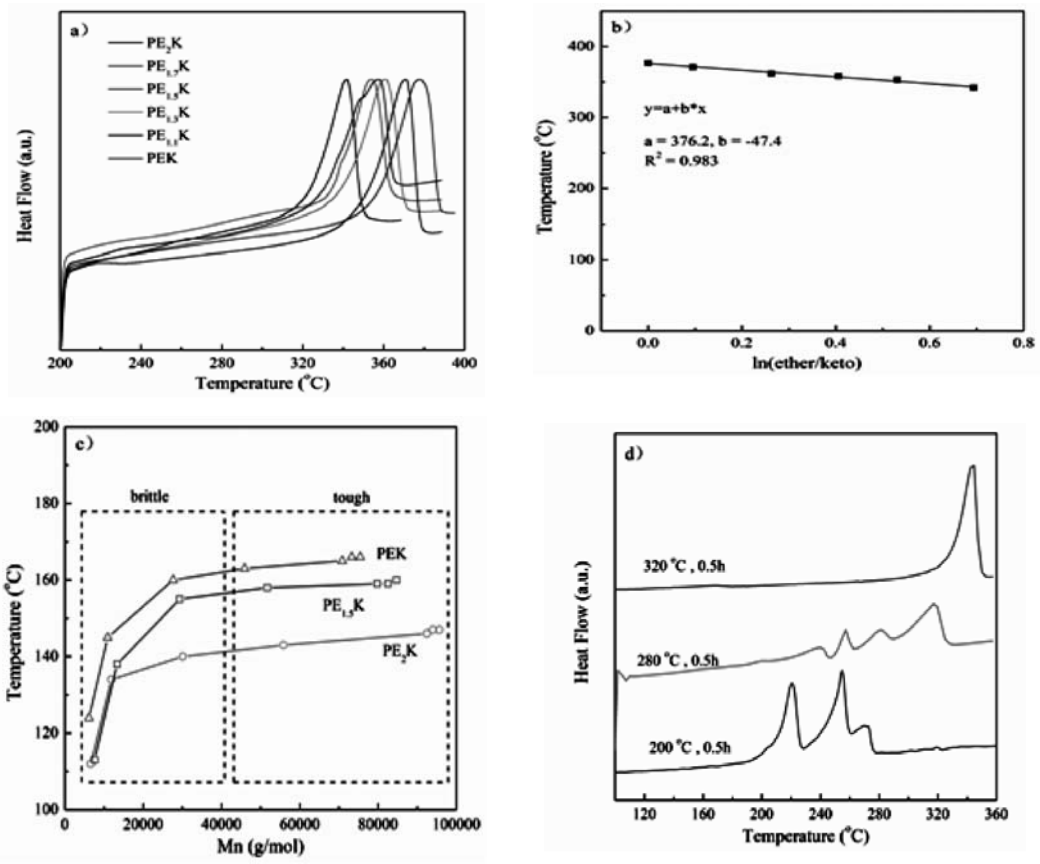

Figure 5. a) Melting curves of the PAEKs with different ether/keto ratios synthesized at the polymerization of 6h at 320°C; b) Dependence of the T_m of the PAEKs as a function of ether/keto ratio; c) Relationship of the T_g of the PAEKs with the molecular weight; d) Melting curves of the PE_2K quenched at different polymerization temperature.

ratios, an empirical formula was proposed to estimate the T_ms of PAEKs. As shown in Fig. 5b, the dependence of T_m with ln(ether/keto) can be well fitted by a straight line with the slope of -47.4 and intercept of 376.2.

T_gs of the PAEKs were affected both by the molecular weights and ether/keto ratios (Fig. 5c and Table 3), and related with the mechanical performances. T_gs of the PAEKs increase rapidly with the molecular weights in the brittle region, and become flat in the tough region, so T_g would a useful index to reflect the mechanical performances of the PAEKs. To avoid the influence of molecular weights, Flory-Fox equation was used to estimate the $T_{g,\infty}$ of the PAEKs.[21]

$$T_g = T_{g,\infty} - K/M_n, \quad (2)$$

$T_{g,\infty}$ is the asymptotic value toward which T_g tends as molecular weight increases, K is a polymer-specific constant. $T_{g,\infty}$s of the PAEKs exhibit similar trends with the ether/keto ratios as the T_ms, which is also attributed to the rigidity of the keto bonds.

Difference of the dependencies of the T_g and T_m on the molecular weight could be explained by styles of chain movement. The glass transition process is an intrachain movement in which the polymer chains start to move, while in the melting process, the polymer chains can intrachain move freely so as to get rid of the interchain entanglement, thus the T_g is more sensitive to the the molecular weight. As can be seen in Fig. 5d, PE_2K quenched at 200 and 280°C were composed

TABLE 3. Thermal properties of the PAEKs with different ether/keto ratios synthesized at the polymerization time of 6h at 320°C.

	$T_{5\%}$ (°C)	T_{max} (°C)	T_m (°C)	ΔH_m (J g^{-1})	T_g (°C)	$T_{g,\infty}$ (°C)
PE_2K	545	565	343	44.9	147	149
$PE_{1.7}K$	548	564	353	47.5	155	
$PE_{1.5}K$	550	569	358	49.1	160	165
$PE_{1.3}K$	563	581	362	49.7	161	
$PE_{1.1}K$	563	583	371	51.3	165	
PEK	565	583	377	53.2	166	169

of oligomers with T_ms lower than 320°C. As it quenched at 320°C, no oligomers with T_ms lower than 320°C were found, and only PE_2K with T_m of 343°C was obtained, indicating the oligomers reacted each other and formed polymers with higher molecular than the critical molecular weight of melting.

Crystallization Behaviors

Non-isothermal crystallization behaviors of the PAEKs were investigated by varying the cooling rate from their melts. Typical non-isothermal crystallization curves of the PAEKs are shown in Fig. 6a, the crystallization temperatures (T_c) and crystallinities (χ) are shown in Table 4. It

can be seen all the PAEKs have good crystallization ability with their χ between 0.35 and 0.45, and no evident trends was found between the ether/keto ratio and χ. All the crystallization curves exhibit asymmetric exothermic peaks, and their T_cs shift to low temperatures with the increase of ether/keto ratios, which indicates the PAEKs with higher ether/keto ratios have lower T_c. For further investigation, the crystallization curves were processed by integral and the relative crystallinities were calculated by the formula as follow[22]:

$$\chi_T = \frac{\int_{T_0}^{T} (dH_c/dT)dT}{\int_{T_0}^{T_\infty} (dH_c/dT)dT}, \quad (3)$$

where T_0 and T_∞ are the temperatures at which the crystallization starts and ends. The plots of relative crystallinity versus temperature are shown in Fig. 6b, all the curves exhibit similar sigmoidal shapes, and induction periods can be found in them, which can be viewed as the nucleation process of the crystallization.

Through inverting the crystallization temperature to crystallization time, Jeziorny's model was used to investigate the crystallization behaviors of the PAEKs and it can be described by the equation as follow[23]:

$$\log[-\ln(1-\chi_T)] = \log(Z_t) + n\log(t), \quad (4)$$

where n is the Avrami exponent and Z_t is the crystallization rate constant related to the nucleation and growth mechanism. To avoid the effect of cooling rate, Z_c is defined to replace Z_t using the formula:

$$\log(Z_c) = \log(Z_t)/\Phi, \quad (5)$$

in which Φ is the cooling rate. It shows the typical plots of $\log[-\ln(1-\chi_T)]$ versus log(t) of the PAEKs in Fig. 6c, all the curves exhibit similar shape which can be divided into two linear parts, corresponding to the primary crystallization and secondary spherulite growth process, respectively.[24] By fitting the two parts, their exponents n_1 (primary) and n_2 (secondary), as well as the Z_c are summarized in Table 4. The n_1 of the PAEKs was about 3~4, which indicates the two or three-dimensional crystallization process during the primary stage. And the n_2 of the peaks was about 2, which might be attributed to the one dimensional lamellae-thickening process of the spherulite. Similar to that of crystallinity, no evident trends between the n_1, n_2, Z_{c1}, Z_{c2} and the ether/keto ratio was found, which might be attributed to the complexity of the polymer crystallization. The crystallization behaviors of the PAEKs are affected by many factors, including crystallization condition, molecular structure, molecular weight and distribution et al.[24]

The activation energies of the PAEKs were calculated by a modified Ozawa method proposed by Doyle.[23] The equation can be described as follow:

$$\log(\Phi) = A - B^*E_a/RT, \quad (6)$$

where A is a constant related with the integral from the crystallization mechanism, B can be chosen to be -0.4567 for most polymers, thus by varying the cooling rate for a fixed χ_T, the Ea for a fixed χ_T can be obtained. Fig. 6d shows the plots of $\log(\Phi)$ versus 1/T for PE_2K at the χ_T of 0.1, 0.3, 0.5, 0.7 and 0.9, respectively. The plots exhibit almost parallel lines with negative slops, the average E_a of PE_2K was calculated to be 550 KJ/mol, which was similar

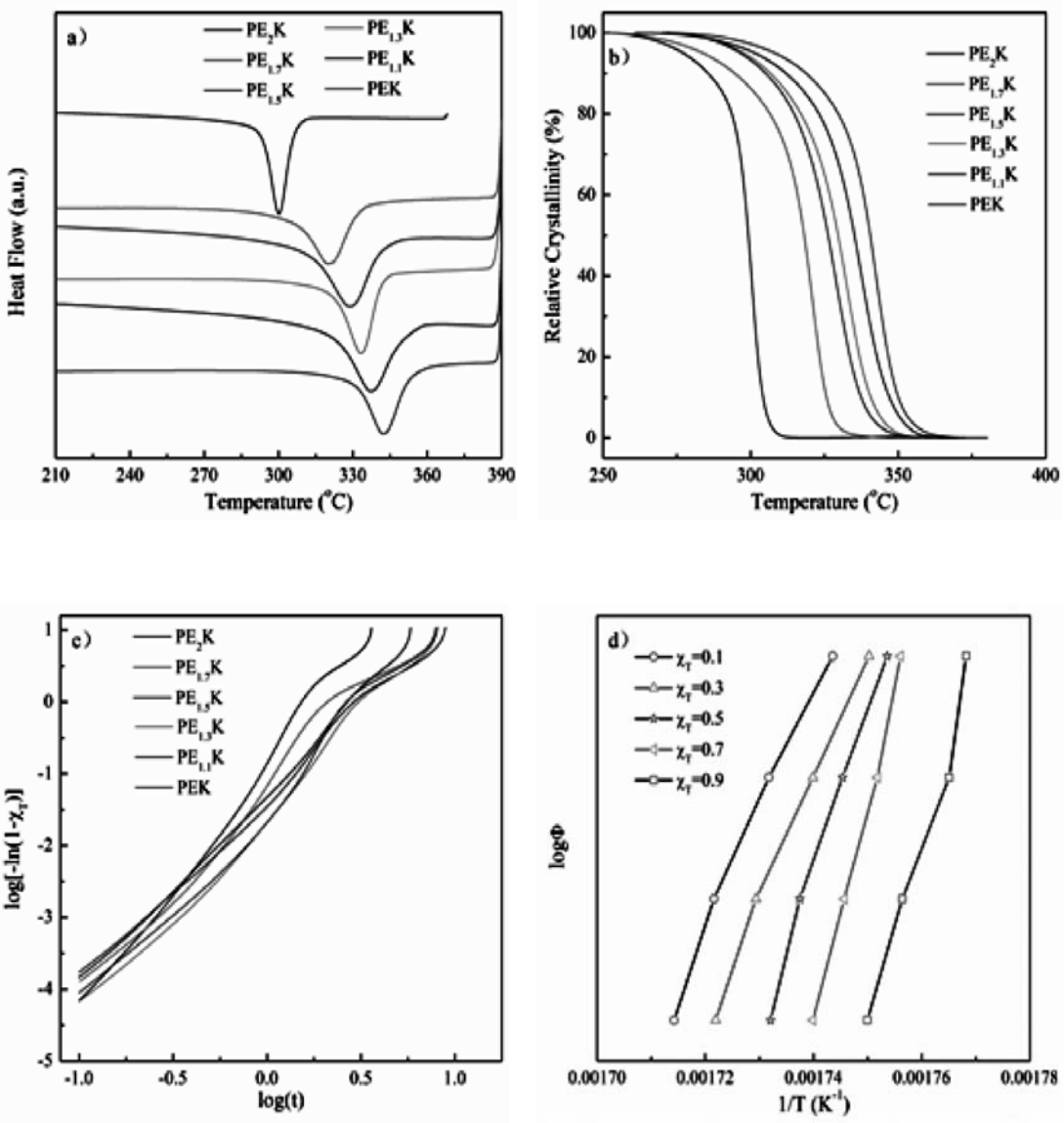

Figure 6. a) Crystallization curves of the PAEKs with different ether/keto ratios synthesized at the polymerization time of 6h; b) Plots of relative crystallinity versus temperature from Fig. 6a; c) Plots of log[-ln(1-χT)] versus log(t) from Fig. 6b; d) Plots of logΦ versus 1/T of the PE_2K.

TABLE 4. Crystallization data of the PAEKs with different ether/keto ratios synthesized at the polymerization time of 6h.

Φ(°C/min)		PE_2K	$PE_{1.7}K$	$PE_{1.5}K$	$PE_{1.3}K$	$PE_{1.1}K$	PEK
2.5	T_c (°C)	307	335	337	341	344	348
	χ (%)	43	42	45	42	45	44
	n_1	4.1	3.6	3.4	2.9	3.7	3.8
	n_2	1.5	1.7	1.2	2.0	1.8	1.9
	Z_{c1}	12.64	13.62	11.55	15.87	14.70	12.16
	Z_{c2}	1.36	1.58	1.66	1.24	1.18	1.29
5	T_c (°C)	303	329	334	336	340	344
	χ (%)	42	42	40	39	43	42
	n_1	3.1	3.5	2.9	3.2	3.0	3.3
	n_2	1.9	1.6	1.7	1.5	1.9	1.8
	Z_{c1}	4.23	4.66	3.87	5.11	3.92	4.03
	Z_{c2}	0.91	0.87	0.89	0.79	0.82	0.93
10	T_c (°C)	300	321	329	333	337	342
	χ (%)	43	41	42	41	44	42
	n_1	3.5	3.3	2.7	2.9	2.7	2.6
	n_2	1.8	1.3	1.5	1.8	2.1	1.5
	Z_{c1}	0.91	0.88	0.86	0.84	0.88	0.84
	Z_{c2}	0.98	0.96	0.94	0.92	0.92	0.94
20	T_c (°C)	291	314	321	325	325	330
	χ (%)	40	40	41	39	42	42
	n_1	4.2	3.9	3.6	3.4	3.8	3.1
	n_2	1.8	1.4	1.6	1.5	2.1	1.9
	Z_{c1}	0.78	0.82	0.75	0.72	0.84	0.68
	Z_{c2}	0.88	0.85	0.83	0.86	0.84	0.87

to Liu's report (545 KJ/mol). The average E_as of $PE_{1.7}K$, $PE_{1.5}K$, $PE_{1.3}K$, $PE_{1.1}K$ and PEK were calculated using the same methods. The results show that they were in the same magnitude and increased slightly with decrease of ether/keto ratios, and PEK had the largest

E_a of 576 KJ/mol among them.

The crystallization behaviors of the PAEKs were also investigated by POM. Fig. 7 shows

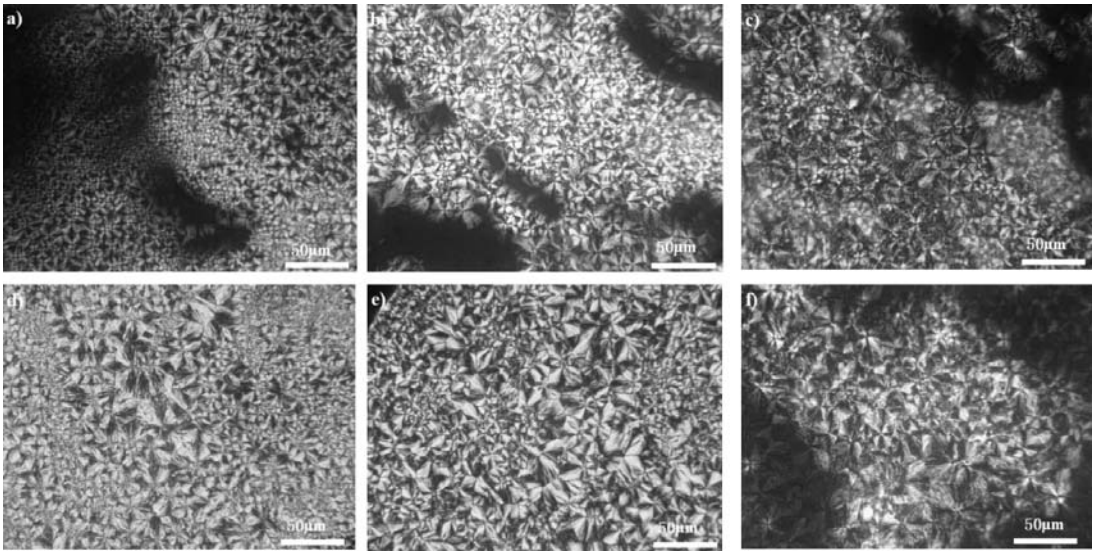

Figure 7. POM images of the PAEKs with different ether/keto ratios synthesized at he polymerization time of 6h. a) PE_2K; b) $PE_{1.7}K$; c) $PE_{1.5}K$; d) $PE_{1.3}K$ and e) $PE_{1.1}K$; f) PEK.

the typical POM images of the PAEKs, all the images exhibit Maltese cross pattern indicating the formation of spherulite. Meanwhile, the sizes of the spherulites increase with the decrease of decrease of ether/keto ratios, PEK shows the largest spherulite. This might be attributed to the relative larger n_2 of PEK (Table 4), which is related to the growth of spherulite.

CONCLUSION

A series of PAEKs with different ether/keto ratios were synthesized by nucleophilic substitution route and their thermal properties, mechanical performances and crystallization behaviors were investigated. T_ms of the PAEKs increased with the decrease of ether/keto ratios and were irrelevant with the temperature, a formula was proposed to estimate the T_ms of PAEKs with different ether/keto ratios. T_gs of the were affected both by the ether/keto ratios and molecular weights, and $T_{g,\infty}$s increased with the decrease of the ether/keto ratios. Tensile strength, flexural strength, impact strength and compressive strength increased as the decreasing of ether/keto ratios, while the elongations decreased with the decrease of the ether/keto ratios. All the PAEKs exhibited excellent thermal stability with 5% weight loss temperature higher than 540°C. All the PAEKs had high crystallinities in the range of 0.35 to 0.45. The non-isothermal crystallization curves exhibited two linear parts when treated by Jeziorny's model, which related to the primary and secondary crystallization processes, and no evident trends between the crystallization behaviors and ether/keto ratios was found. All

the PAEKs exhibited typical Maltese cross pattern, and the sizes of the spherulites increased with the decrease of ether/keto ratios.

ACKNOWLEDGEMENT

The authors gratefully acknowledge the financial support of this work by Natural Science Foundation of China (No. 21975055; U2001222), Science and Technology Planning of Guangdong Province (No. 2019A050510042; 2020B0101030005).

REFERENCES

1. A. R. McLauchlin, O. R. Ghita, L. Savage, *Journal of Materials Processing Technology*, 214 (2014) 75.
2. X. Deng, Z. Zeng, B. Peng, S. Yan and W. Ke, *Materials*, 11 (2018).
3. J. C. Sebileau, S. Lemonnier, E. Barraud, M. F. Vallat, A. Carrado and M. Nardin, *Journal of Applied Polymer Science*, 136 (2019) 47645.
4. G. D. Yu, H. J. Liu, K. Mao, C. C. Zhu, P. T. Wei and Z. H. Lu, *Journal of Tribology-Transactions of the Asme*, 142 (2020) 041702.
5. X. Liao, Y. Sampurno, Y. Zhuang, A. Rice, F. Sudargho, A. Philipossian and C. Wargo, *Microelectronic Engineering*, 98 (2012) 70.
6. J. Liu, Y. Mo, S. Wang, S. Ren, D. Han, M. Xiao, L. Sun and Y. Meng, *Acs Applied Energy Materials*, 2 (2019) 3886.
7. R. Murmu, H. Sutar, *Journal of Polymer Materials*, 35 (2018) 103.
8. Y. Q. Wang, W. D. Muller, A. Rumjahn and A. Schwitalla, *Materials*, 13 (2020).
9. Y. Bao, J. Wang, I. D. Gates, *Journal of Petroleum Science and Engineering*, 153 (2017) 268.
10. M. G. Zolotukhin, D. R. Rueda, F. J. Balta Calleja, M. E. Cagiao, M. Bruix, E. A. Sedova and N. G. Gileva, *Polymer*, 38 (1997) 1471.
11. S. Hamdan, G. M. Swallowe, *Journal of Polymer Science Part B: Polymer Physics*, 34 (1996) 699.
12. Z. Y. Jiang, P. Liu, Q. H. Chen, H. J. Sue, T. Bremner and L. P. DiSano, *Journal of Applied Polymer Science*, 137 (2020) 48966.
13. D. Veazey, T. Hsu, E. D. Gomez, *Journal of Applied Polymer Science*, 136 (2019) 47727.
14. V. L. Rao, P. U. Sabeena, A. Saxena, C. Gopalakrishnan, K. Krishnan, P. V. Ravindran and K. N. Ninan, *European Polymer Journal*, 40 (2004) 2645.
15. K. H. Gardner, B. S. Hsiao, R. R. Matheson and B. A. Wood, *Polymer*, 33 (1992) 2483.
16. D. J. Blundell, J. J. Liggat, A. Flory, *Polymer*, 33 (1992) 2475.
17. W. Q. Zhang, X. L. Wang, G. C. Liu, L. Chen and Y. Z. Wang, *Rsc Advances*, 6 (2016) 84284.
18. J. Devaux, D. Delimoy, D. Daoust, R. Legras, J. P. Mercier, C. Strazielle and E. Nield, *Polymer*, 26 (1985) 1994.
19. Q. S. Lu, Z. G. Yang, X. H. Li and S. L. Jin, *Journal of Applied Polymer Science*, 114 (2009) 2060.
20. L. H. Perng, C. J. Tsai, Y. C. Ling, *Polymer*, 40 (1999) 7321.
21. K. Odriscoll, R. A. Sanayei, *Macromolecules*, 24 (1991) 4479.
22. M. C. Kuo, J. C. Huang, M. Chen, *Materials Chemistry and Physics*, 99 (2006) 258.
23. Y. Hu, P. Xu, H. Gui, S. Yang and Y. Ding, *Rsc Advances*, 5 (2015) 92418.
24. T. X. Liu, Z. S. Mo, S. G. Wang and H. F. Zhang, *Polymer Engineering and Science*, 37 (1997) 568.

Received:

Accepted: